JOURNAL INDIAN ASSOCIATION OF SEDIMENTOLOGISTS ISSN NO 2582 – 2020
Vol. 39, Issue 2, 2022, pp. 17-29
DOI: https://doi.org/10.51710/jias.v39iII.251

Geochemistry and clay mineral studies of Jurassic sedimentary rocks from the Spiti region, Himachal Pradesh, North India

Samar Sultana*, Shaik A. Rashid
Department of Geology, Aligarh Muslim University, Aligarh-202002, India
(Corresponding author*: samaramu.9@gmail.com)

Abstract

An attempt is made in the present study to unravel the provenance, paleoweathering and paleoclimatic conditions of the Jurassic (Spiti Formation) black shales and sandstones from the Spiti region, Tethys Himalaya, using multi proxy approach. The sandstones are subarkose in composition and texturally poorly sorted, subrounded to subangular in shape with moderate spheriocity. The range of the chemical index of alteration (CIA) is 55–90, recorded in the black shales strongly suggests moderate to strong chemical weathering conditions in the source area, which in turn reflect fluctuating climatic conditions prevailing during the deposition of these sediments in Jurassic period in the Spiti region. Geochemical studies reveal that shales are enriched in felsic elements (high SiO_2, Al_2O_3, K_2O) and depleted in mafic components (Fe_2O_3 and MgO).The various geochemical discriminant plots and elemental ratios (SiO_2/Al_2O_3, K_2O/Al_2O_3, Al_2O_3/TiO_2, K_2O/Na_2O, etc.) indicate the rocks to be the product of weathering of felsic rocks. The paleoclimate in the source area seems to be mostly semi-humid. The plot of the samples on the A-CN-K ternary diagram indicates a granitic weathering trend. The X-ray Diffraction studies show that the prominent clay minerals in the Spiti shales are illite, smectite, chlorite, kaolinite and vermiculite along with quartz, muscovite, alkali feldspar, calcite and phosphatic phase.When plotted on the tectonic discrimination diagram, the samples indicate passive margin tectonic setting.

Keywords: Black shales, Spiti region, Tethys Himalaya, Geochemistry, Paleo-climate, Paleo weathering.

Introduction

Due to a variety of factors, the Jurassic epoch in geological history has attained global prominence. Continental configuration, oceanic patterns, and biological systems all changed dramatically throughout the Jurassic period. The Jurassic of India can best be studied in the Spiti region because the Spiti basin records the complete and uninterrupted history of marine sedimentary rocks starting from Eocambrian to Paleogene which were deposited along the northern margin of India.The Spiti area is part of the Tethyan Himalayan mountain range and is located in the Lahaul-Spiti region of Himachal Pradesh in north India. The Tethys Himalayan mountain range has complex geological and geotechnical features and is one of the most seismically and tectonically active mountain ranges in the world. It presents an excellent prospect to comprehend provenance, paleoweathering, paleoclimatic conditions, and plate tectonic investigations throughout te earth history. The Spiti area is where black shales are best preserved. Black shales are common rocks that gained attention throughout the Phanerozoic period on a worldwide scale. The distorted remains of the Indian subcontinent's northern margin are represented by the sedimentary succession of the Tethys Himalaya. Understanding the sedimentary provenance, paleoclimatic state, crustal evolutionary history, and depositional environmental conditions of the sediments requires the fusion of geochemical and petrological approaches (Bhatia & Crook, 1986; Dickinson & Suczek, 1979). Siliciclastic sediments may contain mineralogical and chemical traces that monitor weathering severity in the source area as well as paleoclimate, source rock type, and sediment cyclicity (Nesbitt & Young, 1984; Nesbitt & Young, 1982; Taylor & McLennan, 1985). Geochemical studies of the sedimentary rocks in the Spiti region have received very little attention. However, the stratigraphy and palaeontology of the region have drawn yet more interest. Numerous recent studies have demonstrated that sedimentary geochemistry is a potent tool for identifying and predicting the processes and climate extremes that govern the degree of weathering of the source rocks. As a result, differences in paleo-climate can be determined (Garzanti et al., 2014). The major deciding factors in all of these aspects are the composition of the source rock, the weathering mechanism (Armstrong-Altrin et al., 2004; Taylor & McLennan, 1985) and the tectonic setting of the

sedimentary basin coupled with secondary processes (Wronkiewicz & Condie, 1987). By examining clastic rocks, it is possible to identify continental and oceanic source regions that underwent metamorphism during tectonic activity. This is possible because the source signature persists even after metamorphism (Condie, 1993; Cullers, 2000; McLennan et al., 1993; Nesbitt & Young, 1982). Because of their extremely fine-grained nature, shales take more time to petrographically examine than sandstone does (Blatt, 1985). However, because they are homogenised source representations, shales are preferred in the case of geochemical analysis. The present paper provides the detailed understanding of geochemical proxies and their implications for resolving the paleoweathering condition, provenance, geo-tectonic setting, and paleoclimatic conditions; we present new geochemical data from the Jurassic siliciclastic sequences from the Spiti region, NW Tethys Himalaya, Himachal Pradesh, north India.

Geological setting

The Indian Tethyan Himalayan zone, containing thick sequence of rocks which are predominantly fossiliferous and range in age from the late Precambrian to early Eocene, is developed in three important basins, viz.,Kumaun (Uttarakhand), Kinnaur-Spiti-Zanskar (Himachal Pradesh) and Kashmir (Jammu and Kashmir). These sequences which are best exposed in Spiti - Zanskar region and document depositional history of the Tethys sea over the north facing Indian Plate margin (Bhargava & Bassi, 1998).The Spiti basin along with Zanskar bain is the largest basin in the Indian Tethys Himalaya (Parcha, 2021).The Spiti region is located in the Lahual-Spiti district of Himachal Pradesh. It is flanked by Ladakh and Tibet in the north and northeast, Higher Himalaya in the south, and a nearly undisturbed Phanerozoic succession that spans in age from Eocambrian to Cretaceous with a thickness of more than 7 km (Bhargava, 2008). In the Indian subcontinent, prominent marine Mesozoic rock successions are confined to the Tethyan Himalaya.Based on a number of studies, a broad agreement is achieved to categorise the Jurassic sequences into formations and members of the Lagudarsi Group (Bhargava, 2008; Bhargava & Bassi, 1998).The three formations in ascending order—the Spiti, Giumal, and Chikkim formations make up the Lagudarsi Group in the Spiti region.The geology of Spiti region and sample locations are given in figure 1. Mesozoic rocks of the Spiti region are categorized as Lilang Supergroup, which is divided into five Groups viz. Tamba-kurkur Group, Sanglung Group, Nimoloksa Group, Kioto Group and Lagudarsi Group (Bhargava, 2008). Lagudarsi Group is further subdivided into Spiti, Giumal and Chikkim formations in ascending order (Table.1).The present work is mainly confined to the Spiti Formation of the Lagudarsi Group. Considerable efforts have been made to collect fresh samples from the type localities (along Lingti-Giumal road section) in the Spiti region where the Jurassic rocks are well exposed. The Spiti Formation rests with sharp contact over theTriassic Kioto Formation. It consist of dark Grey to black friable shale, minor chert flakes, local sandstone beds which are calcareous toward the top.In the upper part, the shales gradually become light in colour and have fine flakes of detrital mica.

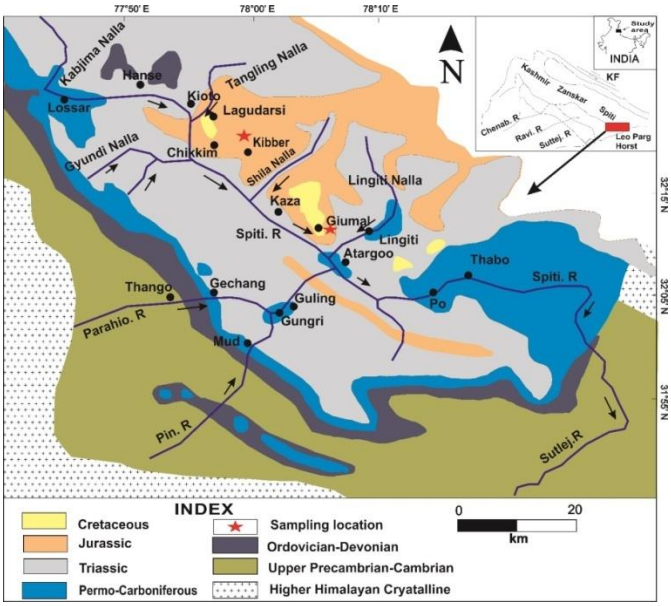

Fig.1.Geological Map of Spiti region (Bagati, 1990).

Table 1.General stratigraphy of the Spiti region (Bhargava, 2008)

Group	Formation	Main Lithology	Age
Lagudarsi	Chikkim	Limestone, Shale	Late Cretaceous
	Giumal	Sandstone, Shale	E-M Cretaceous
	Spiti	Shale	L-Jurassic to E-Cretaceous
Disconformity			
Kioto	Tagling	Limestone, Dolomite	M-Jurassic
	Para	Limestone, Dolomite	L-Triassic
Nimoloksa	Nunuluka	Sandstone, Siltstone, Limestone	L-Triassic
	Alaror	Shale, Sandstone, Limestone	L-Triassic
	Hangrang	Limestone, Dolomite	L-Triassic
	Rangrik	Shale, Sandstone, Limestone	L-Triassic
Sanglung	Rongtong	Dolomite, Limestone	L-Triassic
	Rama	Shale, Sandstone, Limestone	L-Triassic
Tamba- kurkur	Chomule	Limestone	M-L Triassic
	Kaga	Shale, Siltstone, Limestone	M-Triassic
	Mikin	Limestone	E-M Triassic
Disconformity			
Kuling	Gungri	Black Shale, Siltstone	Late Permain
	Gechang	Sandstone, Shale	Early Permain
Disconformity			
`Kanawar	Ganmachidam	Conglomarate, Shale,Sandstone	M-Carb. to E-Permain
	Po	Shale, Sandstone	E-Carb. to M-Carbon
	Lipak	Limestone, Sandstone, Shale	Early carboniferous
	Muth	Quartzite, Sandstone	Late Devonian
Disconformity			
Sanugba	Takche	Limestone, Sandstone, Shale	L-Ordov. L-Silurian
	Thango	Conglomerate	Early Ordovician
Disconformity			
Haimanta	Kunzam La	Sandstone, Shale, Limestone	Cambrian
	Batal	Sandstone, Siltstone, Shale	Precambrian

Note: E-Early, M-Middle, L-Late

Sampling and Analytical techniques

Twenty eight (28) representative samples of shales and six sandstone samples were collected from Giumal village. Agate milling was used to reduce representative samples to a powder with a grain size less than 200 mesh after they had been air dried and roughly crushed. Major oxides concentrations were determined using X-ray Fluorescence Spectrometry (Model name:Axios^{MAX}) at the Birbal Sahni Institute of Paleosciences, Lucknow. The analyses were carried out using pressed powder pellets for the principal components. Internal and international reference standards (such as MBH and SCo-1) were used for calibration. The data precision and accuracy is better than 5 percent and well within the bounds of international norms.The Gazzi-Dickinson method, which successfully reduces the effect of grain size, was used to count 500 points in each thin section for petrographic analyses. Scanning Electron Microscopy (SEM) studies were carried out for the identification of clay minerals in the samples at the University Sophisticated Instrument Laboratory (USIF) at Aligarh Muslim university (AMU), Aligarh, India in order to diagnose and understand the microstructures and diagenetic relationships among the main constituents and the matrix of the studied sediments particularly black shales and different phases. Identification of different phases was done by Bulk powder X-ray diffraction (XRD) analysis of five samples at the Department of Chemistry, AMU, Aligarh.

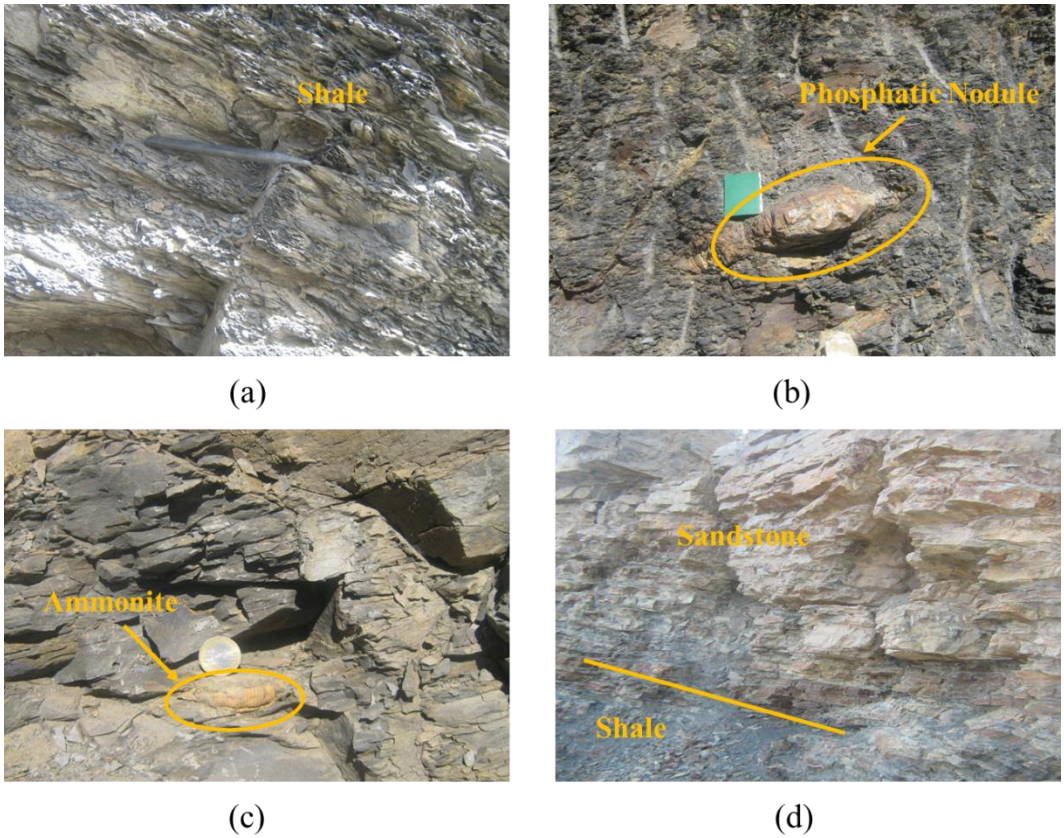

Fig. 2. Field photographs of Spiti Formation (a) Typical Spiti shales near Giumal village section. (b) Spiti black shales showing phosphatic nodules near Giumal village. (c) Photograph showing ammonite bearing Spiti black shales along Giumal village. (d) Spiti sandstone associated with black shales along Giumal village section.

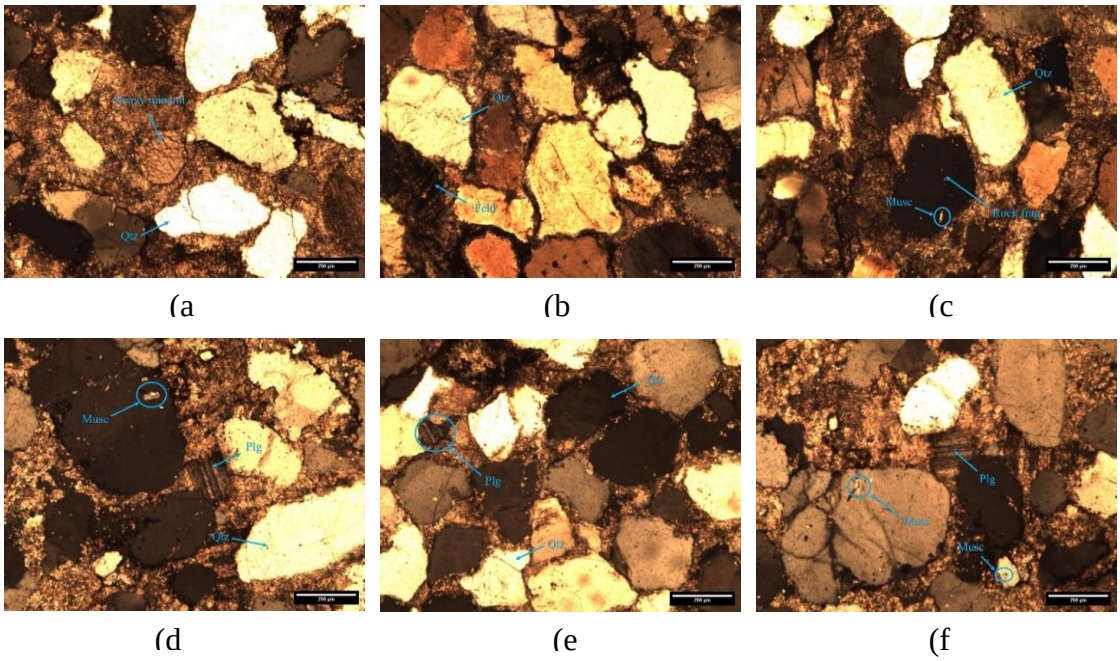

Fig.3.Photomicrograph showing predominantlydetrital monocrystalline quartz and other minerals (plagioclase, K-feldspar, muscovite, heavy minerals) and rock fragments

Results

Thin section analysis

Studying sandstone petrography can help better understand the grain texture, framework, and diagenetic history of sedimentary rocks and depositional history, like the processes involved in transit, deposition, and diagenesis (Lindsey, 1999). Petrographic analysis of Jurassic sandstones of Spiti region reveals that the sandstones are poorly sorted and rounded to subrounded with quartz (80%), feldspar (10%), and clayey matrix. The grain size of the sandstones ranges from fine to coarse. Quartz is predominately monocrystalline with undulose extinction and fractured edges.

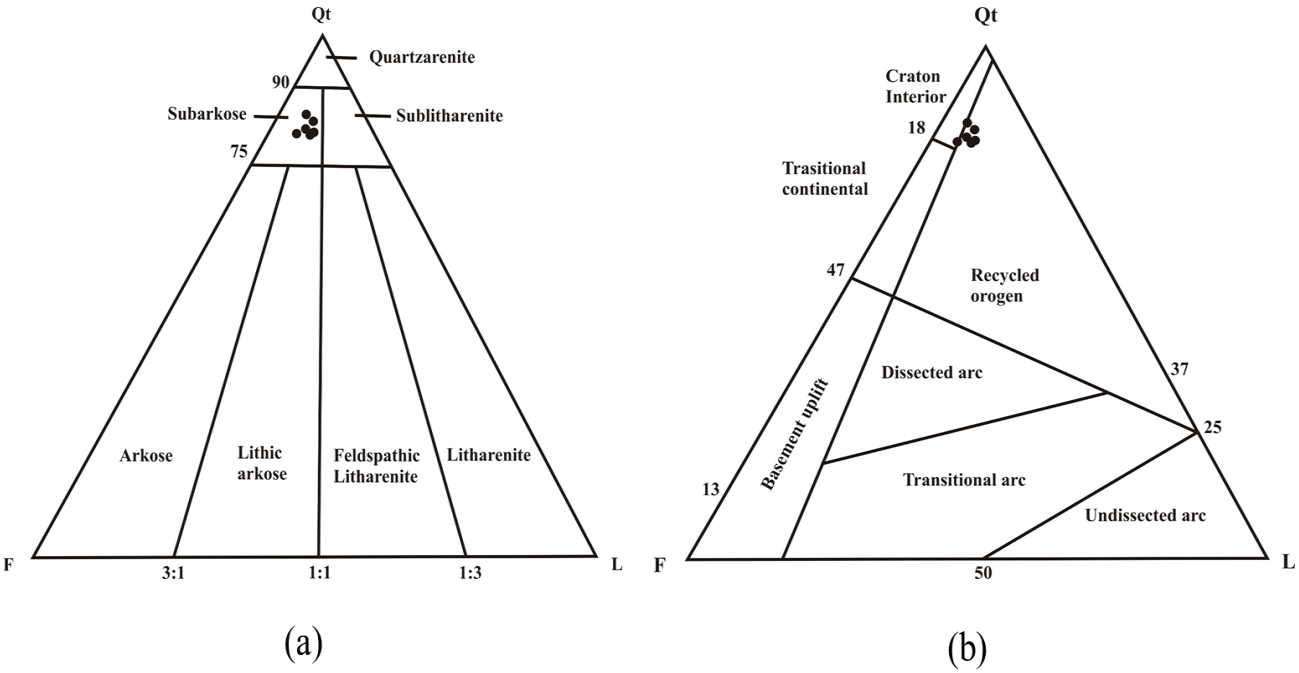

Fig.4. Triangular Qt-F-L plot for (a) classification of Spiti sandstones (Dickinson, 1985) and (b) showing different provenance fields for Spiti sandstones (Dickinson et al.,1979)

Most of the K-feldspars identified in thin sections are microclines i.e., K –feldspar dominating over plagioclase indicating the plutonic rocks (granite) as a dominant source. These sandstones also show presence of mica in the form of muscovite and heavy minerals and rock fragments. For quantitative analysis, approximately 500 points per thin section were counted for determining the modal composition of the samples according to point counting method by Gazzi-Dickinson. The average quartz percentage is about 83, feldspar is 12, and lithic fragments is 6, according to the modal analysis and these sandstones are classified as sub-arkose (Fig.4a). The data of these samples plotted in the Qt-F-L (Qt= total quartz; F: feldspar; L= lithic fragments) provenance diagram (Fig.4b.) show three different types of tectonic regimes as "continental block, magmatic arc and recycled orogen field (Dickinson, 1985; Dickinson & Suczek, 1979), most of these samples plot near Qt apex and in the recycled orogen field indicating that the samples are mineralogically mature and may have been derived from recycled orogen provenance (Fig.4b).

4.2. Clay mineralogy

The clay fraction derived from Spiti shales was subjected to bulk X-ray diffraction analysis, the results show that all of the studied samples mostly contain illite, smectite, kaolinite, vermiculite and chlorite. In addition to these minerals, calcite and phosphates are also identified within the shale rocks. Semi-quantitative analysis indicates that the quartz is the most abundant non-clay mineral, followed by illite, smectite, kaolinite, chlorite and vermiculite clay minerals and the bulk powder XRD patterns of these shales are shown in figure 5. The distribution of clay minerals at different levels of the sequence suggests moderate to intensive chemical weathering of feldspar.

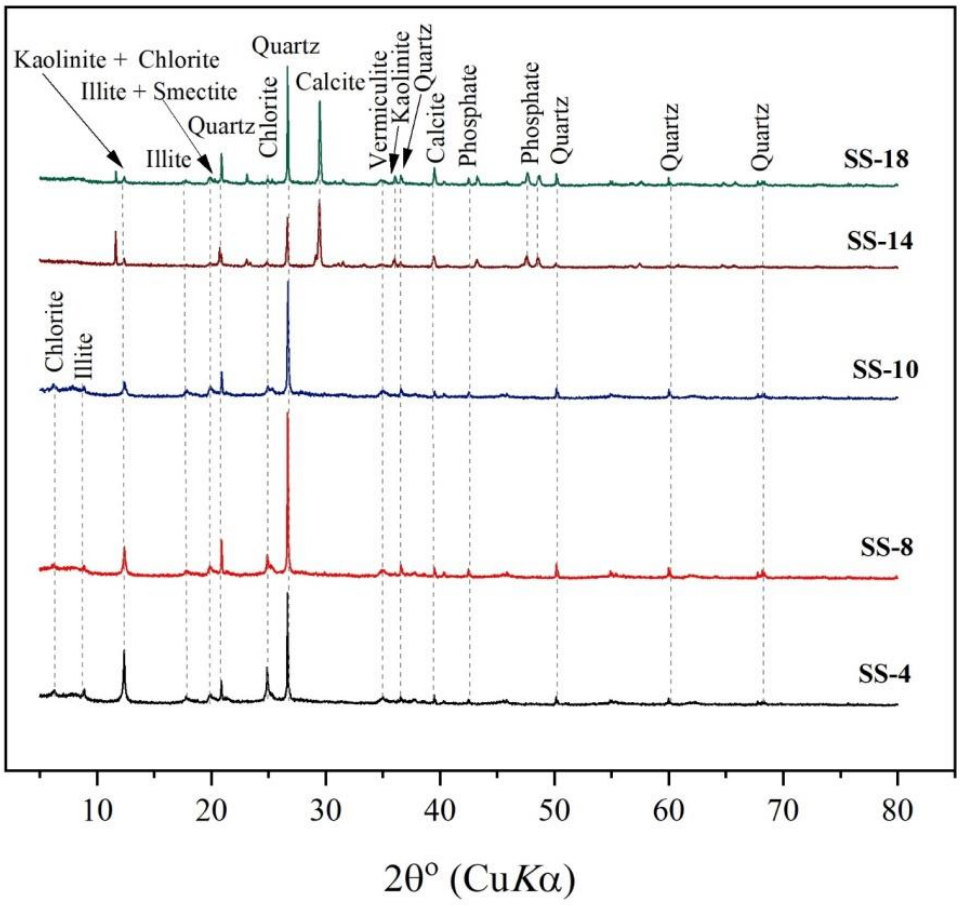

.

Fig.5. The bulk powder X-ray diffraction (XRD) patterns of spiti shales (Cl-chlorite; Q-quartz; I- illite; Ve-vermiculite ; Sm – smectite ; K- kaolinite; P - phosphate and C- calcite).

Geochemistry

The major elemental concentrations and their ratios of the sandstones and shales of present study are given in table 2. The sandstones exhibit high SiO_2 abundance (78-84 wt %) while shales have low range of values (46-65 wt %). The high concentration of SiO_2 in sandstones is due to the high percentage of quartz. Shales possess higher Al_2O_3 (18-28 wt.%), K_2O (1.2 to 5.4wt.%) and Fe_2O_3 (0.4 to 5.8 wt.%). In particular, the Na_2O concentration is less in sandstones (Table 2) as compared to K_2O which indicates the presence of K–rich minerals as compared to Na-rich minerals. This is confirmed by the petrographical study which shows more dominance of K-feldspar than the plagioclase in the sandstones.The apparent control of associated dolomitic limestones may be shown by the noticeably increased quantity of CaO and MgO in some samples, suggesting that CaO is largely absorbed into the calcite or dolomite rather than plagioclase. When compared to upper continental crust (UCC), the studied sandstones show depleted pattern except for SiO_2 and K_2O (Fig. 6). The Spiti shale sample plots on PAAS (post-Archean shales from Australia) diagram show similar values (Fig.7). However, the large enrichment in SiO_2 and Al_2O_3 is noticed indicating the presence of more clay fraction in the samples.

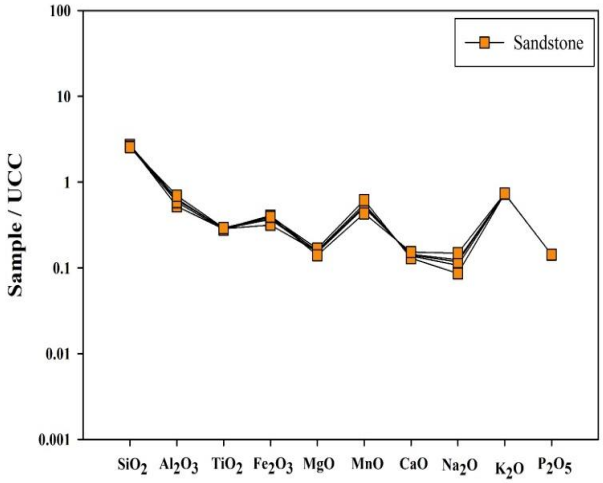

Fig.6. UCC normalized major element pattern of Spiti sandstones (UCC values after Mc Lennan, 2001).

Table 2. Major element concentrations (wt. %) of Spiti shales and sandstones from Spiti region

	Shales																												Sandstones					
	SS1	SS2	SS3	SS4	SS5	SS6	SS7	SS8	SS9	SS10	SS11	SS12	SS13	SS14	SS15	SS16	SS17	SS18	SS19	SS20	SS21	SS22	SS23	SS24	SS25	SS26	SS27	SS28	SPT1	SPT2	SPT3	SPT4	SPT5	SPT6
SiO_2	49.02	49.02	51.19	46.31	49.70	49.32	50.08	50.46	51.10	51.33	53.51	53.89	58.80	58.52	55.42	54.83	52.47	52.62	64.77	65.42	63.89	62.31	61.25	58.72	61.58	60.36	58.33	56.49	79.61	79.09	81.39	82.12	80.87	83.92
Al_2O_3	26.52	28.52	26.63	28.82	27.34	27.65	27.17	27.14	27.15	27.30	25.85	25.72	22.72	22.70	24.35	24.68	26.29	26.59	18.11	18.70	20.18	23.90	24.00	21.74	18.97	21.89	23.29	20.26	4.70	5.61	5.16	4.20	4.99	5.16
TiO_2	1.18	1.18	1.43	1.35	1.13	1.32	1.43	1.31	1.37	1.24	1.31	1.26	0.74	0.78	1.05	0.89	1.00	0.95	0.70	0.73	0.70	1.08	0.97	0.79	0.59	0.86	0.66	0.58	0.12	0.12	0.12	0.12	0.12	0.12
Fe_2O_3	5.39	5.39	5.80	5.66	5.97	5.88	5.75	5.77	5.31	5.17	4.88	4.73	3.75	3.73	4.71	4.72	5.40	5.27	3.01	3.07	1.96	3.06	4.32	3.81	0.42	1.01	1.70	1.46	1.39	1.38	1.43	1.32	1.29	1.11
MgO	1.58	1.58	1.42	1.40	1.58	1.61	1.59	1.61	1.57	1.55	1.50	1.53	0.72	0.71	1.58	1.50	1.33	1.33	1.03	2.02	0.92	0.85	0.82	1.37	1.88	3.07	2.40	3.75	0.22	0.19	0.21	0.21	0.20	0.21
MnO	0.01	0.01	0.00	0.00	0.01	0.01	0.01	0.00	0.01	0.01	0.00	0.01	0.00	0.00	0.01	0.01	0.00	0.01	0.05	1.40	0.72	0.61	0.89	0.47	0.29	0.03	1.02	0.21	0.37	0.26	0.32	0.33	0.30	0.32
CaO	0.30	0.30	0.25	0.22	0.40	0.48	0.51	0.42	0.34	0.31	0.40	0.44	0.60	0.77	0.46	0.70	0.71	0.15	0.26	0.41	0.16	0.16	0.79	0.62	0.52	0.24	0.12	0.39	0.39	0.46	0.42	0.41	0.43	0.42
Na_2O	0.52	0.52	0.54	0.54	0.51	0.52	0.52	0.46	0.82	0.77	0.60	0.63	0.24	0.22	0.24	0.25	0.25	0.28	0.45	0.47	0.27	0.46	0.25	0.18	0.21	0.47	0.29	0.25	0.25	0.43	0.34	0.31	0.36	0.34
K_2O	1.74	1.74	1.71	1.88	1.93	1.88	1.79	1.69	1.85	1.98	1.90	1.84	2.66	2.62	1.13	4.11	3.41	5.40	2.17	2.13	3.67	1.97	2.02	4.99	1.88	5.44	3.33	5.41	2.05	2.07	2.06	2.06	2.06	2.06
P_2O_5	0.08	0.08	0.11	0.11	0.09	0.12	0.18	0.15	0.08	0.08	0.07	0.05	0.32	0.31	0.07	0.09	0.06	0.10	0.14	0.17	0.07	0.04	0.09	0.05	0.15	0.20	0.33	0.19	0.01	0.01	0.01	0.01	0.01	0.01
Total	86.32	88.32	89.09	86.28	88.66	88.78	89.01	89.02	89.60	89.75	90.00	90.10	90.56	90.37	89.01	91.77	90.93	92.71	90.68	94.51	92.53	94.43	95.39	92.74	86.49	93.57	91.47	88.99	89.10	89.62	91.45	91.09	90.63	93.66
CIA	89.31	89.68	89.30	89.66	88.22	88.02	87.97	89.00	87.24	87.28	87.30	87.04	83.88	83.15	90.87	80.08	82.95	80.16	83.54	83.02	81.14	88.28	85.66	76.11	85.06	75.53	84.44	74.38	58.46	59.74	59.15	54.64	58.02	59.15
CIW	96.20	95.31	95.20	95.72	94.58	94.12	93.85	94.67	93.23	93.70	93.80	93.33	93.86	92.80	95.20	93.59	93.88	97.32	93.71	92.50	96.56	95.81	92.90	93.84	93.60	94.78	97.13	94.75	80.75	78.45	79.48	76.91	78.36	79.48
PIA	90.96	91.65	91.48	91.67	89.99	89.81	89.80	90.71	90.55	90.29	89.57	89.47	83.33	82.43	91.85	77.95	81.92	77.23	84.78	84.30	79.20	89.99	85.80	71.46	85.04	71.67	83.74	68.69	45.86	52.30	49.36	39.87	47.74	49.36
WIP	23.43	24.04	24.16	25.46	26.24	26.08	25.25	23.69	27.82	28.33	26.06	25.83	28.96	28.86	16.20	42.29	36.87	52.55	25.35	25.61	35.37	23.44	24.40	48.26	19.56	51.82	32.41	50.27	21.67	23.68	22.71	22.29	22.83	22.48

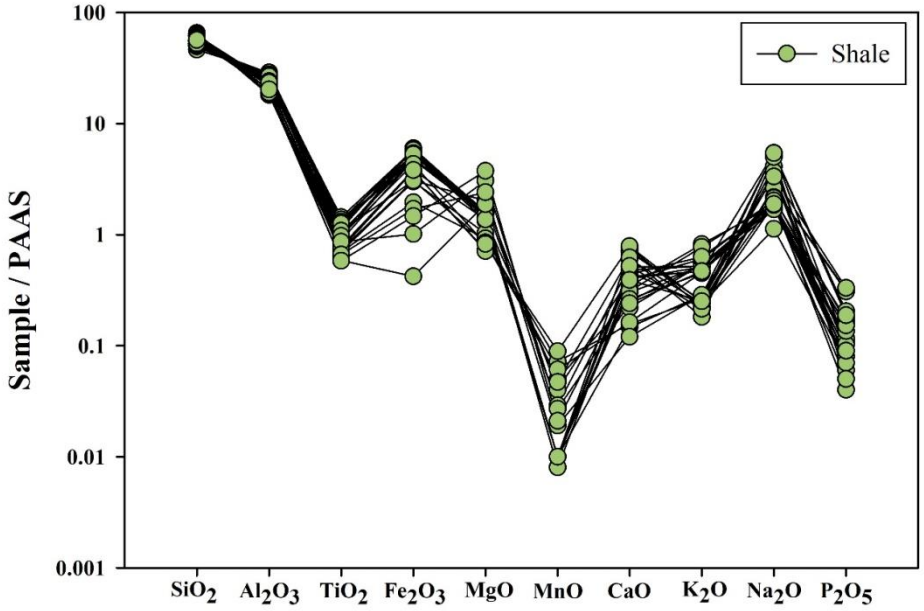

Fig.7. PAAS normalized major element patterns of Spiti shales from Spiti region (PAAS values after Taylor & McLennan, 1985).

Table 3. Correlation matrix of Spiti Shale

	SiO_2	Al_2O_3	TiO_2	Fe_2O_3	MgO	MnO	CaO	Na_2O	K_2O	P_2O_5
SiO_2	1.00									
Al_2O_3	-0.92	1.00								
TiO_2	-0.78	0.87	1.00							
Fe_2O_3	-0.79	0.85	0.83	1.00						
MgO	-0.05	-0.17	-0.20	-0.41	1.00					
MnO	0.65	-0.53	-0.48	-0.49	0.06	1.00				
CaO	0.06	-0.06	-0.11	0.14	-0.25	-0.09	1.00			
Na_2O	-0.49	0.53	0.74	0.46	0.04	-0.28	-0.40	1.00		
K_2O	0.27	-0.35	-0.55	-0.45	0.43	0.09	-0.04	-0.48	1.00	
P_2O_5	0.25	-0.32	-0.44	-0.41	0.22	0.14	0.08	-0.32	0.18	1.00

Table 4. Correlation matrix of Spiti Sandstone

	SiO_2	Al_2O_3	TiO_2	Fe_2O_3	MgO	MnO	CaO	Na_2O	K_2O
SiO_2	1.00								
Al_2O_3	-0.26	1.00							
TiO_2	-0.16	0.75	1.00						
Fe_2O_3	-0.78	0.01	-0.02	1.00					
MgO	0.16	-0.75	-1.00	0.02	1.00				
MnO	0.16	-0.75	-1.00	0.02	1.00	1.00			
CaO	-0.16	0.75	1.00	-0.02	-1.00	-1.00	1.00		
Na_2O	-0.16	0.75	1.00	-0.02	-1.00	-1.00	1.00	1.00	
K_2O	-0.16	0.75	1.00	-0.02	-1.00	-1.00	1.00	1.00	1.00

Because TiO2 is typically dispersed within the clays as separate minerals, such as rutile and anatase, the considerable positive association between TiO_2 and Al_2O_3 (r^2=0.75) suggests that Ti is mostly associated with clays and therefore reflecting its terrigenous origin (Wintsch & Kvale, 1994). It may be clear from the strong positive correlation (Table 4) between CaO and Al_2O_3 (r^2=0.75) that the majority of CaO is not derived from carbonates (von Eynatten et al., 2003).The Spiti sandstones show variable degree of negative correlation for SiO2 vs. Al_2O_3 (r^2= -0.26), TiO_2 (r^2= -0.16), Fe_2O_3 (r^2= -0.78), Na_2O (r^2= -0.16) and K_2O (r^2= -0.16), clearly reflecting a decrease in unstable components (e.g. feldspars and rock fragments) with an increase in mineralogical maturity (Tables 3&4) which may be due to quartz dilution effect. Because the concentrations of Al_2O_3 and SiO_2 are constrained by aluminous clay and quartz contents, respectively, in sedimentary rocks, SiO_2 has a high negative correlation with Al_2O_3 (r^2 = -0.26, Fig.8 a).

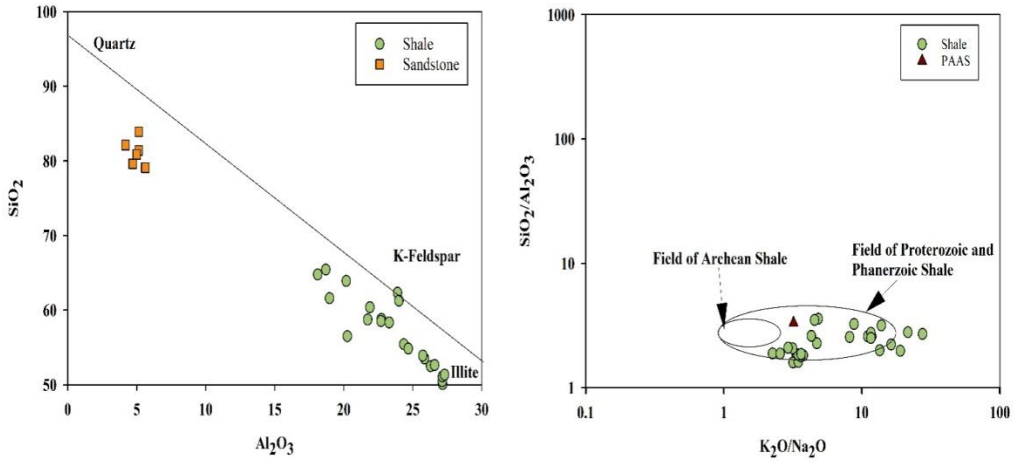

Fig.8. (a) Al_2O_3 –SiO_2 plot for shales and sandstones of Spiti Formation. Note the samples lie near the smooth line and so the sediments can be considered as the product of mixing of two ends (quartz and illite). (b) SiO_2 /Al_2O_3 vs. K_2O/Na_2O plot (Wronkiewicz & Condie, 1987) for Spiti shales and sandstones.

The SiO_2 /Al_2O_3 ratio of the shales lies in between 1.60 to 3.58. On the SiO_2 /Al_2O_3 versus K_2O/Na_2O bivariate diagram (Fig. 8b) the shales, as expected, plot in the field of Proterozoic-Phanerozoic shales (Fig. 8b). At a given K_2O/Na_2O ratio, the related sandstones have greater SiO_2 /Al_2O_3 ratios than the shales, indicating a quartz dilution effect. According to Cox et al., (1995) major element composition of shales is controlled mainly by clay minerals rather than the non-clay silicate phases. K_2O/Al_2O_3 ratio suggests how much alkali feldspar against plagioclase and clay minerals may have been associated with the original shales. The K_2O/Al_2O_3 ratio of minerals, from high to low values are represented by alkali feldspars (0.4 – 1), illite (0.3), other clay minerals (0) (Cox et al., 1995). Sediments with K_2O/Al_2O_3 larger than 0.5 indicates that there was a substantial amount of alkali feldspar in the original samples compared to other minerals; while those with K_2O/Al_2O_3 less than 0.4 indicates that there was minimal alkali feldspar in the original samples (Cox et al., 1995). The Spiti shales and sandstones have an average K_2O/Al_2O_3 = 0.17(range, 0.05 – 0.49). The overall low K_2O/Al_2O_3 ratios of the Spiti Formation suggest minimal involvement of alkali feldspar relative to other minerals in the original samples and strongly support the fact that K_2O addition to the shales has not taken place. The K_2O/Na_2O ratio of Spiti shales ranges from 2.25 to 27.6, which is higher than the value of different post-Archean shale standards (3.1–3.5, (Condie, 1993). The P_2O_5 and SiO_2 concentrations, on the other hand, range from 0.05 to 0.33 wt % and 46 to 65 wt %, respectively.

Discussion

Classification

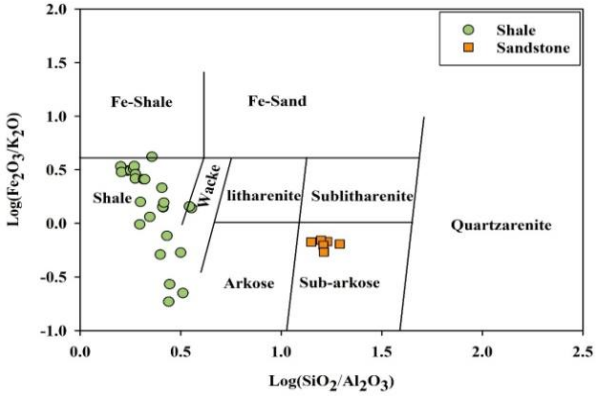

Fig.9 (a).Chemical classification diagram of the Spiti samples (Herron, 1988)

The chemical composition of the classes quartz arenite, graywacke, and arkose can be characterized using the ratios (silica, alumina, alkali oxides, magnesium and iron oxides), which can be represented using two-dimensional diagrams with varying degrees of success (Lindsey, 1999). A fourth sandstone class, lithic arenite, is compositionally diverse; several classifications with modest success, but lithic-arenites can not be identified with great reliance by chemical composition alone. Based on the geochemical studies, sandstones are classified as subarkose (Fig. 9 a) according to Herron (1988) classification. While it is also clear from the chemical classification diagram (Pettijohn et al., 1972), i.e., log (SiO_2/ $A1_2O_3$) vs. log (Na_2O/K_2O) diagram that the sandstones are classified as subarkose in nature (Fig. 9 b).

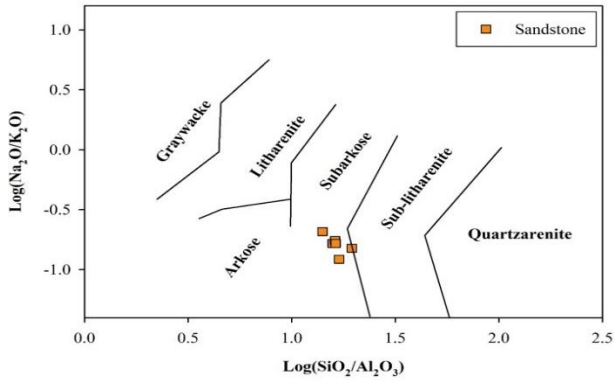

Fig. 9(b). Chemical classification diagram of Spiti sandstones (Pettijohn et al., 1972).

Paleoweathering

The intensity and duration of weathering in clastic sedimentary rocks can be estimated by examining the association between alkali and alkaline elements (Nesbitt et al., 1996). The Chemical Index of Alteration (CIA) (Nesbitt & Young, 1982) is a well-established way of assessing the degree of source rock weathering among the known indices of weathering. The Plagioclase Index of Alteration (PIA) (Fedo et al., 1995), Chemical Index of Weathering (CIW) (Harnois 1988), and Weathering Index of Parker (WIP) (Parker, 1970) can all be used to analyse source rock weathering and elemental redistribution during diagenesis.

CIA = {Al_2O_3 / (Al_2O_3+ CaO* + Na_2O + K_2O)} x 100

PIA = {(Al_2O_3 – K_2O) / (Al_2O_3 – K_2O + CaO*+ Na_2O)} x 100

CIW = {Al_2O_3 / (Al_2O_3 + CaO* + Na_2O)} x 100

WIP = {(2Na_2O / 0.35) + (MgO / 0.9) + (2K_2O / 0.25) + (CaO* / 0.7)} x 100

The major oxides are represented in molar proportions in the above equations, and CaO* represents the quantity of CaO integrated in the silicate fraction only. According to the WIP definition, the smaller WIP values indicate stronger chemical weathering, which is opposite to CIA values (Hamdan & Bumham, 1996). CIA, PIA, WIP and CIW values of Spiti samples were calculated and presented in table 2. The calculated CIA values are 55 -60 (avg. 58) and 74- 91 (avg. 85) for the Spiti sandstones and black shales, respectively suggesting that the source rocks underwent moderate to intense chemical weathering. Whereas, PIA values for the Spiti sandstones and shales are 40-52 and 69-92 (avg. 47and 85), respectively indicating moderate to intense chemical weathering. Similarly, CIW and WIP values also indicate moderate to intense degree of chemical weathering in the source area. The CIA values are also shown in Al_2O_3-(CaO+Na_2O)-K_2O ternary plot (Fedo et al., 1995; Nesbitt & Young, 1984) commonly known as the 'A–CN–K' diagram (Fig. 10) to classify the composition of the provenance and weathering trends. This diagram is used to understand the rate of weathering of K –feldspar and plagioclase (Ca–Na feldspar). As a result, CaO and Na_2O are preferentially leached during weathering compared to K_2O, allowing the weathering trend to follow the A–CN join.Weathering removes CaO, Na_2O, and K_2O from source rock, making the trend parallel to the A–K junction. The A–CN–K ternary diagram is used to plot the Spiti samples,with the majority of the samples placed above the feldspar tie line. It has been observed that the studied samples had undergone moderate to intense chemical weathering based on their weathering patterns.

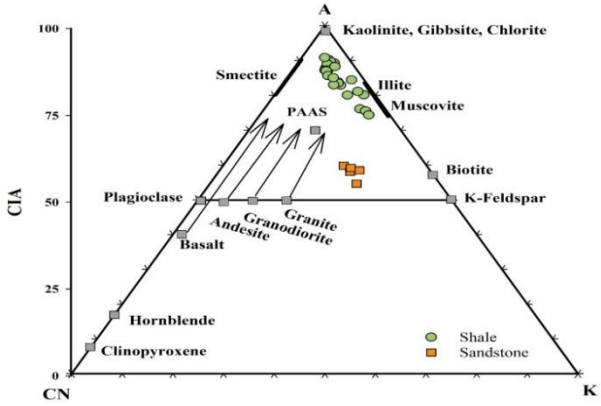

Fig.10. A–CN-K diagram (after Nesbitt & Young, 1984) of Spiti sediments. Arrows showing the weathering trends of basalt, andesite, granodiorite and granite.

Provenance characteristics

The objective of provenance study is to evaluate the evolution and the nature of source rocks. The chemical composition of siliciclastic sedimentary rocks is based on the chemical composition of their provenance, and this principle has been used to describe the source rocks from which the studied sedimentary

rocks were formed (Cullers, 2000; Taylor & McLennan, 1985; Kanhaiya et al., 2018; Verma et al., 2012). Thus, geochemical markers of clastic sediments were used to determine provenance attributes. Diagenesis, weathering and hydraulic sorting all have a consequence on the geochemical composition of the sediments. However, major oxides such as Al_2O_3 and TiO_2 (as well as their ratios i.e., Al_2O_3 /TiO_2), are significant immobile elements that provide significant indications about the source region (Taylor and McLennan 1985; Hayashi et al., 1997). For mafic rocks, the Al_2O_3 /TiO_2 ratio ranges from 3-8, for intermediate rocks from 8-21, and for felsic rocks from 21-70 (Hayashi et al., 1997). High Al_2O_3 /TiO2 values in the analyzed samples (18.5–35.3) for Spiti shales and (36-47) for Spiti sandstone show that the Spiti sediments were derived from intermediate and felsic igneous provenances. Knowing the importance of Al and Ti in provenance studies, (Mc Lennan et al., 1993) devised a bivariate discrimination diagram for Al_2O_3 vs.TiO_2 to determine the provenance of siliciclastic rocks. The Spitui shales data got plotted along the granodiorite to 3granite+ 1basalt trend line in the diagram (Fig. 11).

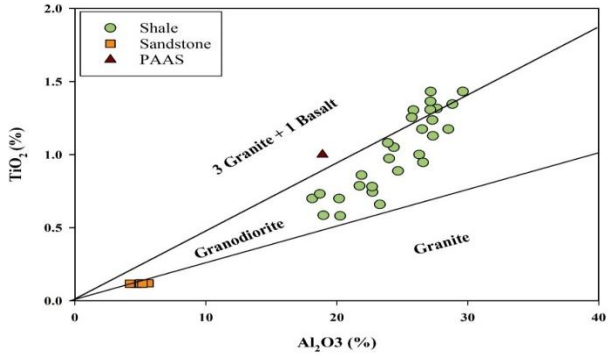

Fig.11. TiO_2 (wt%) vs. Al_2O_3 (wt%) bivariate diagram (Mc Lennan et al., 1993) for Spiti silliciclastic sedimentary rocks. The "granite line" and "3 granite + 1basalt line" (Schieber, 1992).

Overall major element geochemical characteristics of the Spiti sediments shows high SiO_2, Al_2O_3, K_2O contents and having low MgO, Fe_2O_3, CaO and Na_2O concentrations suggesting a dominant felsic source with minor mafic input.

5.4. Tectonic setting

Many studies reveal that the chemical composition of the siliciclastic rocks are influenced by the plate tectonic setting of their source regions and thus siliciclastic rocks from distinct tectonic settings have terrain specific geochemical signatures (Bhatia & Crook, 1986; Roser & Korsch, 1986). As a result, sediments from various tectonic settings show a wide range of geochemical features.

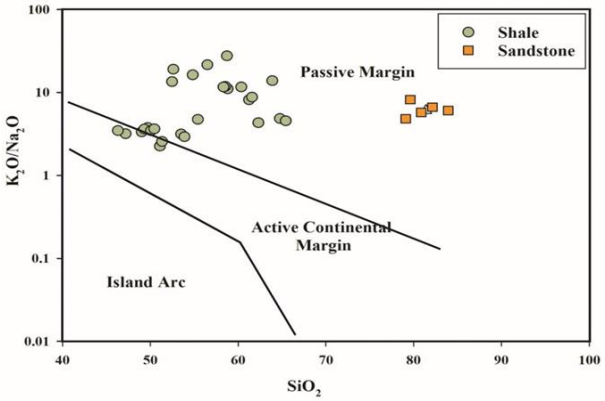

Fig.12. Tectonic setting diagram of Spiti shales and sandstones (Roser & Korsch, 1986)

By using log (K_2O/Na_2O) vs SiO_2, Roser & Korsch (1986) suggested major element based discrimination diagrams to create the tectonic setting of older sedimentary basins. The Spiti shales and sandstones are plotted in the passive margin tectonic setting while few samples lies in the active continental margin setting (Fig. 12). According to Roser & Korsch (1986) passive margin sediments are largely quartz-rich derived from plate interiors or stable continental areas and deposited on passive continental margins or in intracratonic basins .

Paleoclimatic conditions

To desipher the paleoclimatic condition of siliciclastic rocks, Suttner & Dutta (1986) presented a binary diagram SiO_2wt. % vs (Al_2O_3 +K_2O+Na_2O) wt. %. In the (Fig.13), the Spiti sandstones lie in a semi-humid climatic region.

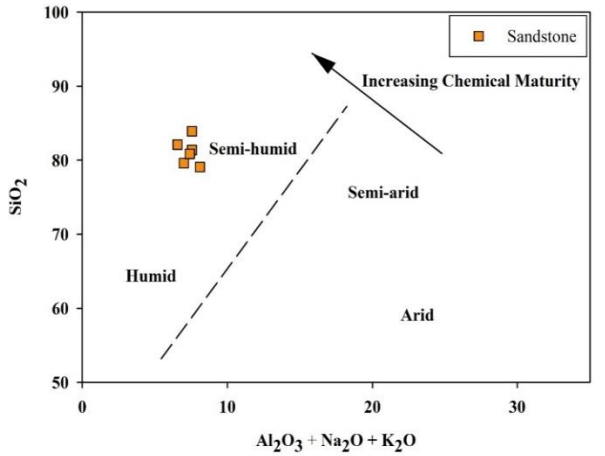

Fig.13. SiO_2Vs (Al_2O_3 +K_2O+Na_2O) palaeoclimate discrimination diagram (after Suttner & Dutta, 1986) of the Spiti sandstones.

Conclusions

A Jurassic siliciclastic sedimentary sequence from the Spiti Formation comprising of shales and sandstones were studied in the present study..On the basis of petrographical and geochemical studies, the sandstones are classified into sub-arkose type.

The bulk powder XRD (X-ray diffraction) studies of the black shales of the Spiti Formation show the dominance of illite, smectite, kaolinite, chlorite and vermiculite as clay minerals suite with silica and phosphatic phases.

The chemical weathering indices (CIA, PIA, CIW, and WIP) and the ACNK ternary diagrams reveal moderate to intense chemical weathering in the source area of Spiti Formation.

The Spiti rocks lie mainly in the passive tectonic setting and indicate semi humid paleoclimate conditions in the Spiti region during Jurassic period.

Discriminant function diagrams and Qt-F-L ternary diagram suggest dominantly felsic (including quartzose sedimentary and granitic rocks) provenance for the Spiti sedimentary sequence.

Acknowledgment:

The authors sincerely thank the chairperson Department of Geology, A.M.U., Aligarh for providing necessary facilities and continuous support. We also thank Dr. Indra Sen, IIT Kanpur and Dr. Anupam Sharma, BSIP, Lucknow for extending the analytical facilities.

References

Armstrong-Altrin, J. S., Lee, Y. I., Verma, S. P., & Ramasamy, S. (2004). Geochemistry of Sandstones from the Upper Miocene Kudankulam Formation, Southern India: Implications for Provenance, Weathering, and Tectonic Setting. *Journal of Sedimentary Research*, *74*(2), 285–297. https://doi.org/10.1306/082803740285

Bagati, T. N. (1990). Lithostratigraphy and facies variation in the Spiti basin (Tethys), Himachal Pradesh, India. *Journal of Himalayan Geology*, *1*(1), 35–47.

Bhargava, O. N. (2008). An updated introduction to the Spiti geology. *Journal of the Palaeontological Society of India*, *53*(2), 113–128.

Bhargava, O. N., & Bassi, U. K. (1998). *Geology of Spiti-Kinnaur Himachal Himalaya* (Vol. 124). Geological Survey of India.

Bhatia, M. R., & Crook, K. A. W. (1986). Trace element characteristics of graywackes and tectonic setting discrimination of sedimentary basins. *Contributions to Mineralogy and Petrology*, *92*(2), 181–193. https://doi.org/10.1007/BF00375292

Blatt, H. (1985). Provenance studies and mudrocks. *Journal of Sedimentary Research*, *55*(1), 69–75.

Condie, K. C. (1993). Chemical composition and evolution of the upper continental crust: Contrasting results from surface samples and shales. *Chemical Geology*, *104*(1–4), 1–37.

Cox, R., Lowe, D. R., & Cullers, R. L. (1995). The influence of sediment recycling and basement composition on evolution of mudrock chemistry in the southwestern United States. *Geochimica et Cosmochimica Acta*, *59*(14), 2919–2940. https://doi.org/10.1016/0016-7037(95)00185-9

Cullers, R. L. (2000). The geochemistry of shales, siltstones and sandstones of Pennsylvanian–Permian age, Colorado, USA: Implications for provenance and metamorphic studies. *Lithos*, *51*(3), 181–203.

Dickinson, W. R. (1985). Interpreting provenance relations from detrital modes of sandstones. In *Provenance of arenites* (pp. 333–361). Springer.

Dickinson, W. R., & Suczek, C. A. (1979). Plate Tectonics and Sandstone Compositions1. *AAPG Bulletin*, *63*(12), 2164–2182. https://doi.org/10.1306/2F9188FB-16CE-11D7-8645000102C1865D

Fedo, C. M., Wayne Nesbitt, H., & Young, G. M. (1995). Unraveling the effects of potassium metasomatism in sedimentary rocks and paleosols, with implications for paleoweathering conditions and provenance. *Geology*, *23*(10), 921–924.

Garzanti, E., Vermeesch, P., Padoan, M., Resentini, A., Vezzoli, G., & Andò, S. (2014). Provenance of passive-margin sand (Southern Africa). *The Journal of Geology*, *122*(1), 17–42.

Hamdan, J., & Bumham, C. P. (1996). The contribution of nutrients from parent material in three deeply weathered soils of Peninsular Malaysia. *Geoderma*, *74*(3–4), 219–233.

Hayashi, K.-I., Fujisawa, H., Holland, H. D., & Ohmoto, H. (1997). Geochemistry of 1.9 Ga sedimentary rocks from northeastern Labrador, Canada. *Geochimica et Cosmochimica Acta*, *61*(19), 4115–4137.

Herron, M. M. (1988). Geochemical classification of terrigenous sands and shales from core or log data. *Journal of Sedimentary Research*, *58*(5), 820–829.

Kanhaiya, S., Singh, B. P., & Singh, S. (2018). Mineralogical and geochemical behavior of sediments solely derived from Bundelkhand granitic complex, central India: Implications to provenance and source rock weathering. *Geochemistry International*, *56*(12), 1245–1262.

Lindsey, D. A. (1999). *An evaluation of alternative chemical classifications of sandstones*. US Geological Survey.

McLennan, S. M. (2001). Relationships between the trace element composition of sedimentary rocks and upper continental crust. *Geochemistry, Geophysics, Geosystems*, *2*(4).

McLennan, S. M., Hemming, S., McDaniel, D. K., & Hanson, G. N. (1993). Geochemical approaches to sedimentation, provenance, and tectonics. In *Geological Society of America Special Papers* (Vol. 284, pp. 21–40). Geological Society of America. https://doi.org/10.1130/SPE284-p21

Nesbitt, H. W., & Young, G. M. (1984). Prediction of some weathering trends of plutonic and volcanic rocks based on thermodynamic and kinetic considerations. *Geochimica et Cosmochimica Acta*, *48*(7), 1523–1534.

Nesbitt, H. W., Young, G. M., McLennan, S. M., & Keays, R. R. (1996). Effects of chemical weathering and sorting on the petrogenesis of siliciclastic sediments, with implications for provenance studies. *The Journal of Geology*, *104*(5), 525–542.

Nesbitt, Hw., & Young, G. M. (1982). Early Proterozoic climates and plate motions inferred from major element chemistry of lutites. *Nature*, *299*(5885), 715–717.

Parcha, S. K. (2021). Stratigraphy and the Fossil record of the Palaeozoic and Mesozoic Tethyan sequences of North-western Himalaya. *Himalayan Geology*, *42*(1), 1–68.

Parker, A. (1970). An index of weathering for silicate rocks. *Geological Magazine*, *107*(6), 501–504.

Pettijohn, F. J., Potter, P. E., & Siever, R. (1972). Sand and Sandstone. Springer-Verlag, Berlin Heidelberg New York. In *Pp 618 Pitman WC*.

Roser, B. P., & Korsch, R. J. (1986). Determination of tectonic setting of sandstone-mudstone suites using SiO2 content and K2O/Na2O ratio. *The Journal of Geology*, *94*(5), 635–650.

Schieber, J. (1992). A combined petrographical—Geochemical provenance study of the Newland Formation, Mid-Proterozoic of Montana. *Geological Magazine*, *129*(2), 223–237.

Scholle, P. A. (1979). Constituents, Textures, Cements, and Porosities of Sandstones and Associated Rocks. *US Geological Survey, Published by the American Association of The American Association of Petroleum Geologists Foundation. Tulsa, Oklahoma, USA 193p*.

Suttner, L. J., & Dutta, P. K. (1986). Alluvial sandstone composition and paleoclimate; I, Framework mineralogy. *Journal of Sedimentary Research*, *56*(3), 329–345.

Taylor, S. R., & McLennan, S. M. (1985). *The continental crust: Its composition and evolution*.

Verma, M., Singh, B. P., Srivastava, A., & Mishra, M. (2012). Chemical behavior of suspended sediments in a small river draining out of the Himalaya, Tawi River, northern India: Implications on provenance and weathering. *Himal Geol*, *33*, 1–14.

Von Eynatten, H., Barcelo-Vidal, C., & Pawlowsky-Glahn, V. (2003). Composition and discrimination of sandstones: A statistical evaluation of different analytical methods. *Journal of Sedimentary Research*, *73*(1), 47–57.

Wintsch, R. P., & Kvale, C. M. (1994). Differential mobility of elements in burial diagenesis of siliciclastic rocks. *Journal of Sedimentary Research*, *64*(2a), 349–361.

Wronkiewicz, D. J., & Condie, K. C. (1987). Geochemistry of Archean shales from the Witwatersrand Supergroup, South Africa: Source-area weathering and provenance. *Geochimica et Cosmochimica Acta*, *51*(9), 2401–2416.

Zuffa, G. G. (1985). Optical analyses of arenites: Influence of methodology on compositional results. In *Provenance of arenites* (pp. 165–189). Springer.